J. Mol. Model. **2000**, *6*, 467 – 476

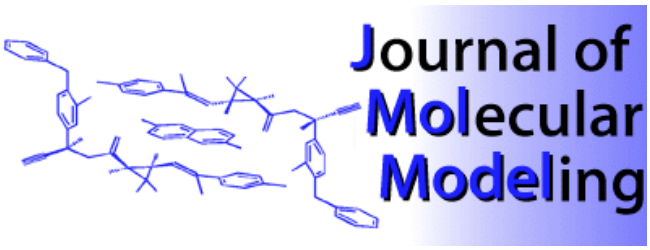

FULL PAPER

© Springer-Verlag 2000

Interaction Energy Analysis of Nonclassical Antifolates with Human Dihydrofolate Reductase

Conrad Pitts[1], Donnell Bowen[2], and William M. Southerland[1]

[1]Department of Biochemistry and Molecular Biology, Howard University College of Medicine, 520 "W" Street NW, Washington, D. C. 20059. Phone: (202) 806-9711; Fax: (202) 806-5784. E-mail: wsoutherland@fac.howard.edu

[2]Department of Pharmacology, Howard University College of Medicine, Washington, D. C. 20059

Received: 30 November 1999/ Accepted: 29 March 2000/ Published: 27 June 2000

Abstract The x-ray structure of the PTX:NADPH:L22F human mutant DHFR ternary complex was used as a structural template to generate structural models for the following wild type DHFR complexes: PTX:DHFR:NADPH, TMP:DHFR:NADPH, EPM:DHFR:NADPH, and TMQ:DHFR:NADPH. Each of these complexes were subsequently modeled in a 60 Å cube of explicit water and minimized to a rms gradient of from $1.0\text{-}3.0\cdot10^{-5}$ kcal·Å^{-1}. For each complex, interaction energies were calculated for the antifolate interaction with each of the following: the DHFR binding site residues, the entire DHFR protein, the solvated complex (containing DHFR, NADPH, and solvent water), water alone, and NADPH. Additionally, each antifolate was subdivided into distinct substructural regions and interaction energy calculations were performed in order to evaluate their contributions to overall antifolate interaction. Each antifolate showed its most stable interaction with the solvated complex. Substructural regions which consisted of a nitrogen containing aromatic ring system contributed most to the stability of the antifolate interactions, while the hydrocarbon aromatic rings, methoxy, and ethoxy groups showed much less stable interaction energies. Since the different substructural regions of nonclassical antifolates differ in their contributions to overall antifolate binding, those substructural regions which exhibit relatively unfavorable interaction energies may constitute important targets in the design of improved DHFR inhibitors.

Keywords Antifolates, Interaction energy, DHFR binding

Introduction

Dihydrofolate reductase is an important therapeutic target in the treatment of cancer, bacterial and fungal infections, and opportunistic infections associated with AIDS [1-8].

Correspondence to: W. M. Southerland

Dihydrofolate reductase (DHFR) inhibitors (antifolates) may be grouped into two categories (classical and nonclassical) according to their structural properties. Classical antifolates have structures similar to folic acid, the natural substrate for DHFR. Folate analogs generally consist of a pteridine moiety, a aryl moiety, and a glutamyl group. These substances are readily glutamated by the intracellular folylpolyglutamyl synthetase [9-14]. In fact, the polyglutamated form of these agents are primarily responsible for DHFR inhibi-

tion in vivo [15-18]. However, Nonclassical antifolates are not folate analogs. They are not susceptible to glutamation and are much less water soluble than the folate analogs. Nonclassical antifolates generally consist of a diaminopyrimidine moiety and an aryl moiety, or a pteridine moiety and a aryl moiety. Nonclassical antifolates include but are not limited to trimethoprim (TMP), piritrexim (PTX), trimetrexate (TMQ), and epiroprim (EPM). TMP is an effective inhibitor of bacterial dihydrofolate reductases [1, 19]. PTX [20-25] and TMQ [3,5,6,26] inhibit mammalian DHFRs. TMQ also has activity against fungal DHFR [4]. EPM has been explored as a treatment for Pneumocystis carinii and Toxoplasma gondii infections [27-29].

The antifolate substructural moieties may be viewed as structural modules which collectively makeup the complete antifolate structure and subsequently determine the binding properties of the intact antifolate. It was of interest to evaluate the contributions of the antifolate substructural regions to the overall antifolate interaction. In this report we employ molecular modeling and subsequent interaction energy calculations to examine the interaction of TMP, EPM, PTX, and TMQ and their corresponding substructural regions to human wild type dihydrofolate reductase.

Methods

The x-ray structure of the piritrexim (PTX):NADPH:L22F human mutant DHFR complex [30] was obtained from the Protein Databank [31]. The mutant DHFR component of the complex was converted to wild type DHFR by changing the PHE side chain at position 22 to LEU using the mutate facility of QUANTA [32], the molecular modeling software from Molecular Simulations Inc. As a result, the structural model for the PTX:NADPH:wild type DHFR complex was generated. Using the molecular editor facility of QUANTA [32], the PTX component of this complex was converted to EPM, TMP, and TMQ, respectively, which resulted in the generation of molecular models for the following three additional complexes: EPM:DHFR:NADPH, TMP:DHFR:NADPH, and TMQ:DHFR:NADPH. The complexes were then modeled inside a 60 Å cube of explicit water. Water molecules were generated based on the TIP3P model [33]. The density of water in the cube was approximately 1.0 gram/milliliter. Each solvated complex was minimized to a rms gradient of from $1.0\text{-}3.0\cdot10^{-5}$ kcal·Å^{-1} using the Adopted-Basis Newton Raphson algorithm in charmm [34]. After minimization, the DHFR binding site residues for each complex were defined as those DHFR residues which contained at least one atom that was 3.7 Å or closer to an antifolate atom. Distances between antifolate atoms and DHFR atoms were calculated using the COOR DIST function in charmm. Charmm was used to calculate the Van der Waals and electrostatic components of the interaction energies. Interaction energies reported here represents the sum of the Van der Waals and electrostatic components. Minimizations were performed using a Silicon Graphics dual processor Octane workstation or a four processor Silicon Graphics origin200 server.

Results

Table 1 shows the DHFR binding site residues for each complex. As can be seen, each antifolate interacts with a slightly

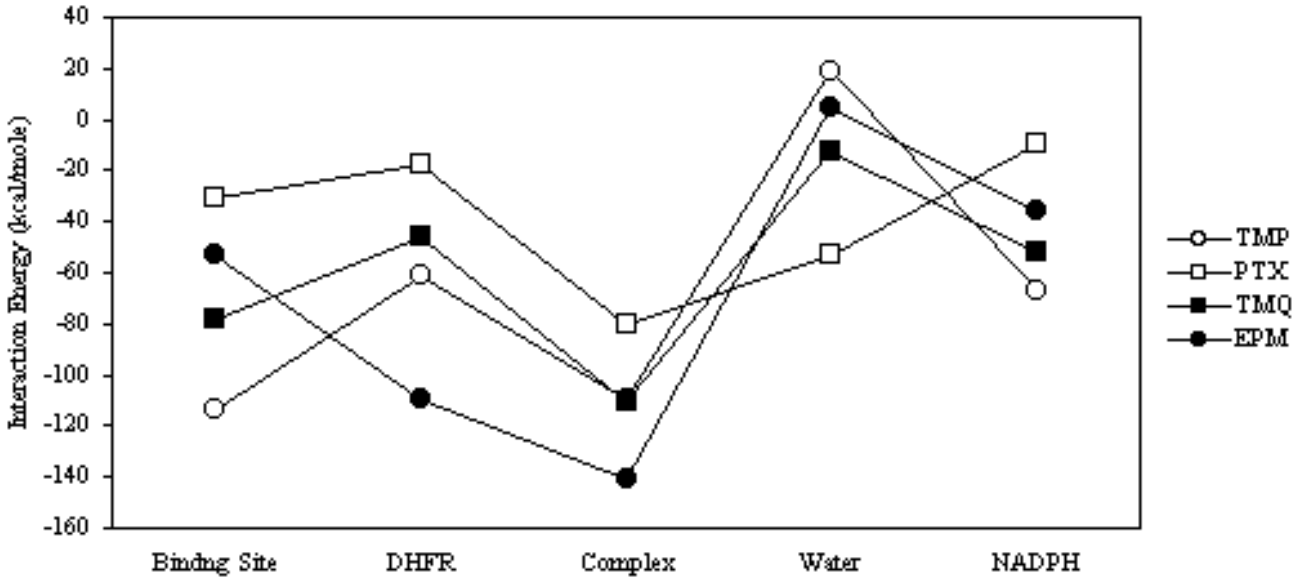

Figure 1 *Interaction energy analysis of TMP, PTX, TMQ, and EPM*

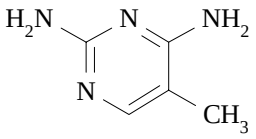

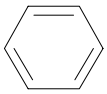

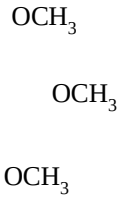

TMP

2,4-Diaminopyrimidinyl-5-methyl Aryl Methoxy

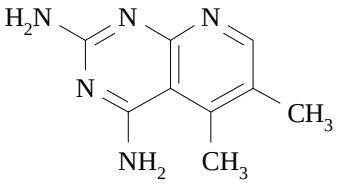

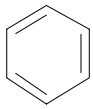

PTX

Heterocyclic Aryl Methoxy

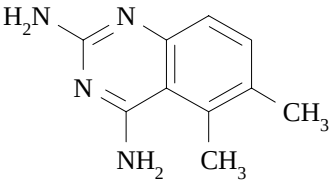

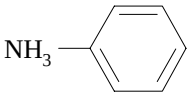

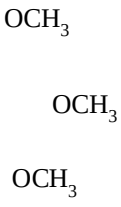

TMQ

Heterocyclic Arylamino Methoxy

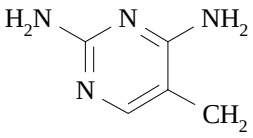

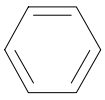

EPM

2,4-Diaminopyrimidinyl-5-methyl Aryl Ethoxy Pyrrol

Figure 2 *Subdivision of TMP, PTX, TMQ, and EPM into their substructural regions*

Table 1 *Comparison of Binding Site Residues for Each Antifolate/DHFR Complex*

DHFR Complex	Binding Site Residues									
TMP	VAL8	ASP21	LEU22	GLU30	PHE31	PHE34	ILE60	PRO61	VAL115	
EPM	VAL8	ALA9	ASP21	LEU22	PHE31	PHE34	ILE60	PRO 61	ASN64	LEU 67
	VAL115									
TMQ	ILE7	VAL8	LEU22	GLU30	PHE31	PHE34	ILE60	ASN64	LEU 67	VAL115
PTX	VAL8	ALA9	LEU22	GLU30	PHE31	PHE34	ILE 60	PRO 61	LEU 67	VAL115

different set of residues. However, the following residues: VAL8, LEU22, PHE31, PHE34, ILE60, and VAL115 are involved in the binding of each nonclassical antifolate studied. Figure 1 compares the interaction energies of each antifolate with its binding site residues (binding site), the DHFR protein only (DHFR), the solvated complex (consisting of DHFR and NADPH and water) (complex), water only (water), and NADPH. TMQ and TMP showed similar interaction patterns with the binding site and complex interactions showing the most stability. For EPM the DHFR and complex interactions were the most stable and for PTX the most stable interactions were complex and water. While the complex interaction was important for each antifolate, these observations indicate that each individual component of the complex, (i. e. binding site, DHFR, water, and NADPH) contributes to the overall binding of the antifolate and that the contribution of each component of the complex may differ for different antifolates.

In order to evaluate the contribution of antifolate substructural moieties to overall antifolate interaction, each antifolate was divided into distinct substructural regions (Figure 2). The interaction energy of each substructural region was calculated and compared with that of its corresponding intact antifolate. Additionally, most substructural regions were further divided into groups of carbon, nitrogen, or oxygen atoms and the interaction energies of these groups of atoms were calculated. Those substructural regions which consisted only of carbon and hydrogen atoms were not further subdivided. The interaction energies of hydrogen atoms were included in the calculation of the interaction energies of the carbon, nitrogen, or oxygen atoms to which they were bonded.

Figure 3a compares the interaction energies of TMP and its 2,4-diaminopyrimidinyl-5-methyl, aryl, and methoxy substructural regions. As can be seen, the pattern of interaction energies observed for TMP and 2,4-diaminopyrimidinyl-5-methyl are very similar. Additionally, the 2,4-diaminopyrimidinyl-5-methyl interactions are generally more stable than those of the aryl and methoxy groups. Figure 3b shows that the nitrogen and carbon atoms of the 2,4-diaminopyrimidinyl-5-methyl moiety exhibit opposing interaction patterns and that the carbon atoms are the primary contributors to the stability of the 2,4-diaminopyrimidinyl-5-methyl interaction. However, the 2,4-diaminopyrimidinyl-5-methyl nitrogen atoms showed a more favorable interaction with water. In Figure 3c, the methoxy groups and their oxygen atoms show similar patterns, while the carbon atoms showed an opposing pattern. The methoxy carbons atoms show more favorable interactions with binding site and NADPH, while the methoxy oxygen atoms show more favorable interactions with DHFR.

Figure 4a compares the interaction energies of PTX and its substructural regions. It is very clear that the heterocyclic region of PTX is the major contributor to the stability of the PTX interaction. The aryl and methoxy regions show much less stable interactions and their patterns of interaction were substantially different from those exhibited by PTX and the heterocyclic region. Figure 4b shows that the carbon and nitrogen atoms of the PTX heterocyclic region make strikingly opposing contributions to the overall heterocyclic interaction. The carbon atoms exhibit more stable interactions with the binding site, DHFR, complex, and NADPH, while the nitrogen atoms show more stable interactions with water. In the case of the methoxy component of PTX (Figure 4c), the pattern exhibited by the carbon atoms is similar to that observed for the entire methoxy group.

The stability of the EPM interaction is primarily derived from the pyrrol, ethoxy, and 2,4-diaminopyrimidinyl-5-methyl interactions (Figure 5a). Aryl generally showed much less stable interactions. Figure 5b shows that the carbon and nitrogen atoms of 2,4-diaminopyrimidinyl-5-methyl exhibit opposing interaction patterns with the pattern exhibited by the carbon atoms coinciding with that exhibited by the overall 2,4-diaminopyrimidinyl-5-methyl group. The overall 2,4-diaminopyrimidinyl-5-methyl group and its carbon atoms make more favorable interactions with complex and NADPH than observed for the 2,4-diaminopyrimidinyl-5-methyl nitrogen atoms. Except for the binding site and NADPH interactions, the ethoxy oxygen atom interactions appear slightly more stable than those of the ethoxy carbon atoms (Figure 5c).

Reminiscent of the heterocyclic region of PTX, the heterocyclic region of TMQ is clearly the major contributor to the stability of the TMQ:complex interaction (Figure 6a). The carbon atoms of the heterocyclic group are the primary contributors to the heterocyclic interactions and they exhibit a pattern of interaction similar to that observed for the overall heterocyclic moiety (Figure 6b). The carbon atoms of the TMQ arylamino group showed an interaction pattern very similar to that of the overall arylamino group (Figure 6c). In the case of the methoxy groups of TMQ, the carbon and oxy-

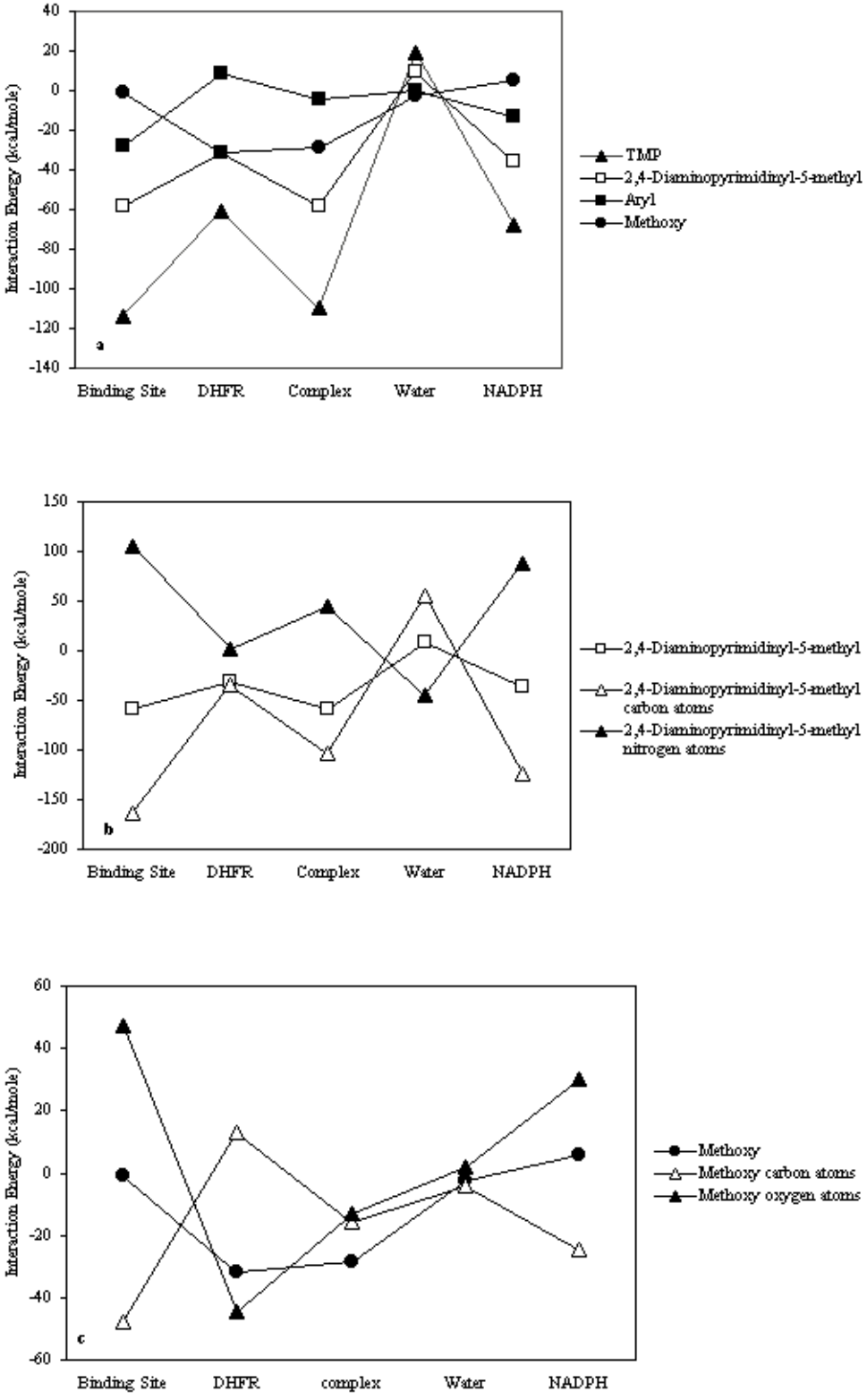

Figure 3 *Interaction energy analysis of TMP and its substructural regions.* **a.** *Comparison of TMP and its substructural regions.* **b.** *Comparison of the 2,4-diaminopyrimidinyl-5-methyl region of TMP with its carbon and nitrogen atoms.* **c.** *Comparison of the methoxy region of TMP with its carbon and oxygen atoms*

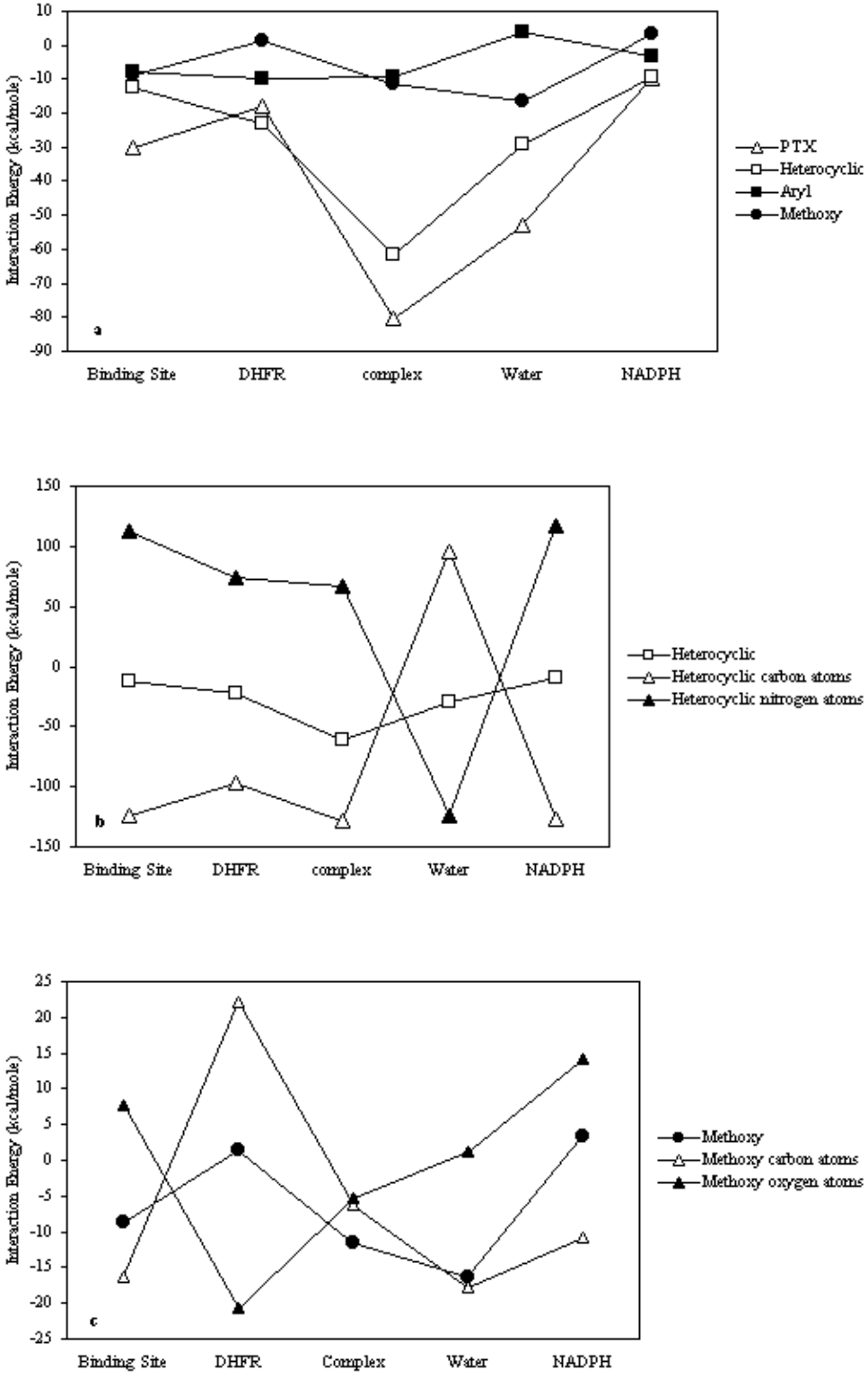

Figure 4 *Interaction energy analysis of PTX and its substructural regions.* **a.** *Comparison of PTX and its substructural regions.* **b.** *Comparison of the heterocyclic region of PTX with its carbon and nitrogen atoms.* **c.** *Comparison of the methoxy region of PTX with its carbon and nitrogen atoms*

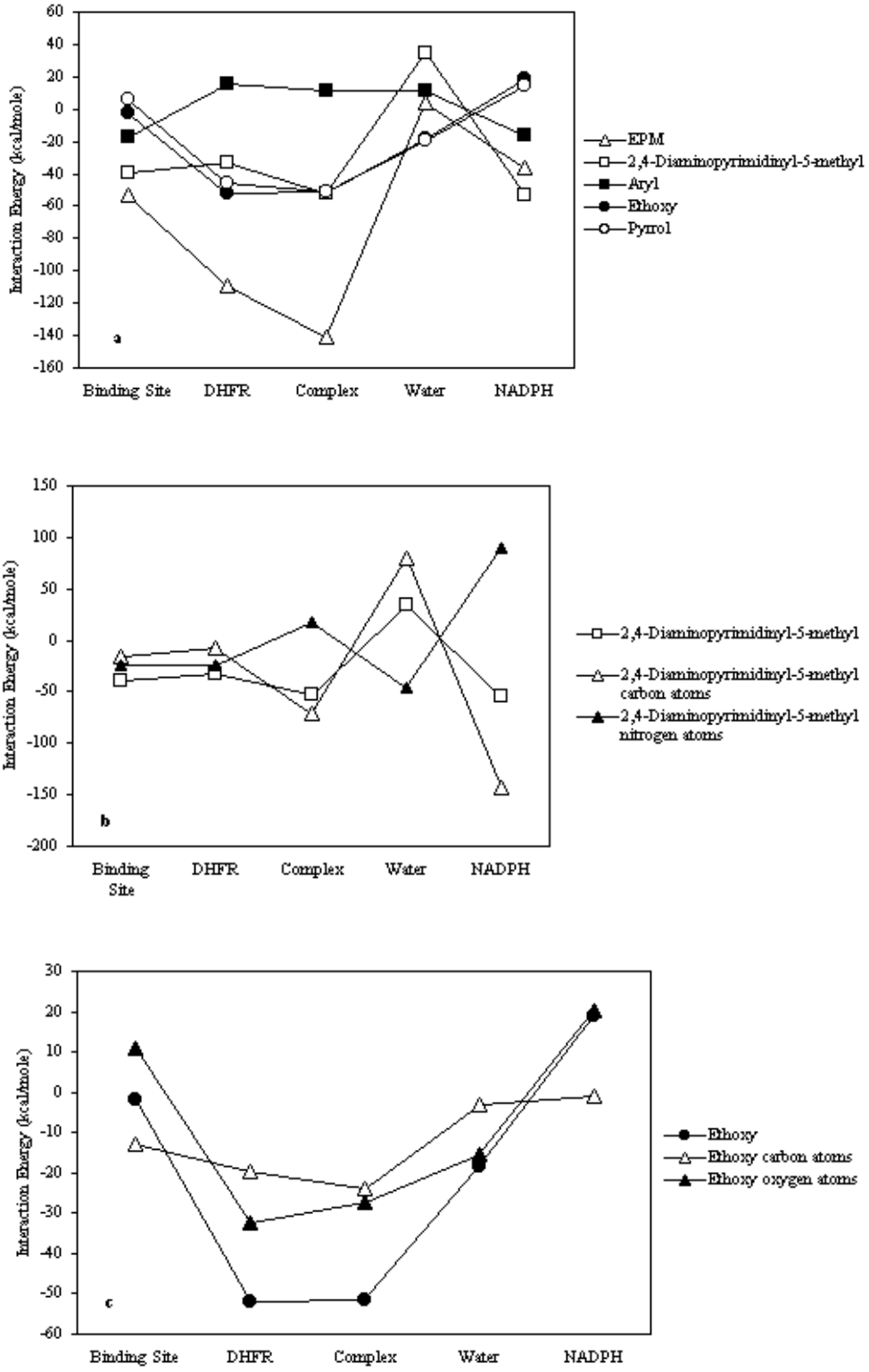

Figure 5 *Interaction energy analysis of EPM and its substructural regions.* **a.** *Comparison of EPM and its substructural regions.* **b.** *Comparison of the 2,4-diaminopyrimidinyl-5-methyl region of EPM with its carbon and nitrogen atoms.* **c.** *Comparison of the ethoxy region of EPM with its carbon and oxygen atoms*

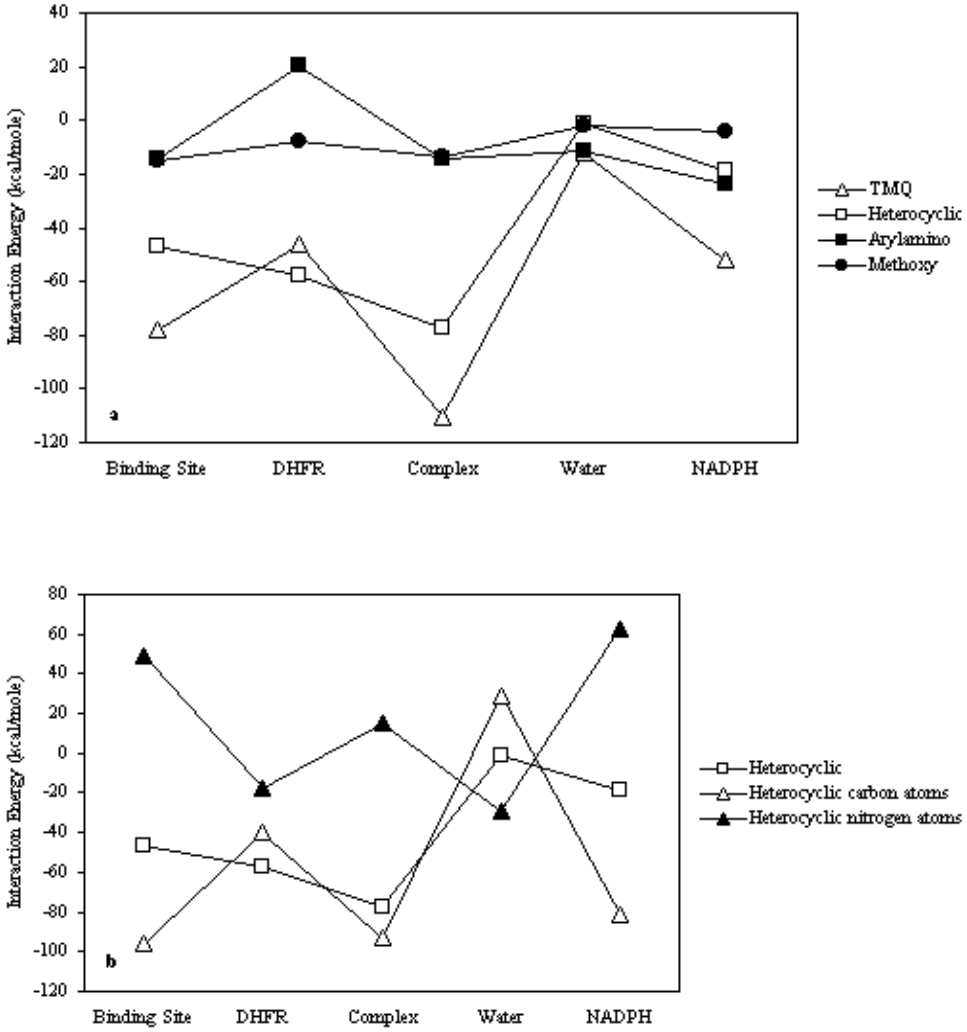

Figure 6 (continued next page) *Interaction energy analysis of TMQ and its substructural regions.* **a.** *Comparison of TMQ and its substructural regions.* **b.** *Comparison of the heterocyclic region of TMQ with its carbon and nitrogen atoms*

gen atoms show opposing patterns of interactions which are distinctly different from that observed for the overall methoxy group (Figure 6d). However, the oxygen atoms seem to contribute slightly more to the overall methoxy stability.

Discussion

The nonclassical antifolates reported here consists of complex molecular structures that may be subdivided into simpler structural subregions. Evaluation of the interaction energies for the substructural regions revealed that for each antifolate a particular substructural region(s) serves as the primary contributor to the stability of the overall antifolate interaction.

The nitrogen containing aromatic ring systems of TMP, PTX, and TMQ, consistently showed the greatest contribution to the stability of overall antifolate interaction. The aryl groups of TMP and EPM and the aryl and arylamino groups of PTX and TMQ contain only aromatic carbons and their associated hydrogens. However, the latter subregions also contains a non-aromatic amino nitrogen attached to the aromatic hydrocarbon ring (Figure 2). It should be noted that these aryl rings showed much less favorable interactions. These observations suggests that the combination of nitrogen and carbon atoms in an aromatic environment is important to stable ligand binding. However, in those aromatic rings which contain both nitrogen and carbon atoms, it is the carbon atoms that exhibit the more stable interaction energies. In general, the methoxy, ethoxy, and aryl groups contributed less to the stability of the antifolate interactions.

The ethoxy, 2,4-diaminopyrimidinyl-5-methyl, and pyrrol groups of EPM showed similar interaction energies with DHFR and complex. These groups appear to exert their primary effect on EPM binding via interaction with the DHFR protein.

Observations reported here reveal that the different antifolate substructural regions differ in their contributions to overall antifolate binding. Those antifolate substructural regions which exhibit unfavorable or poor interaction ener-

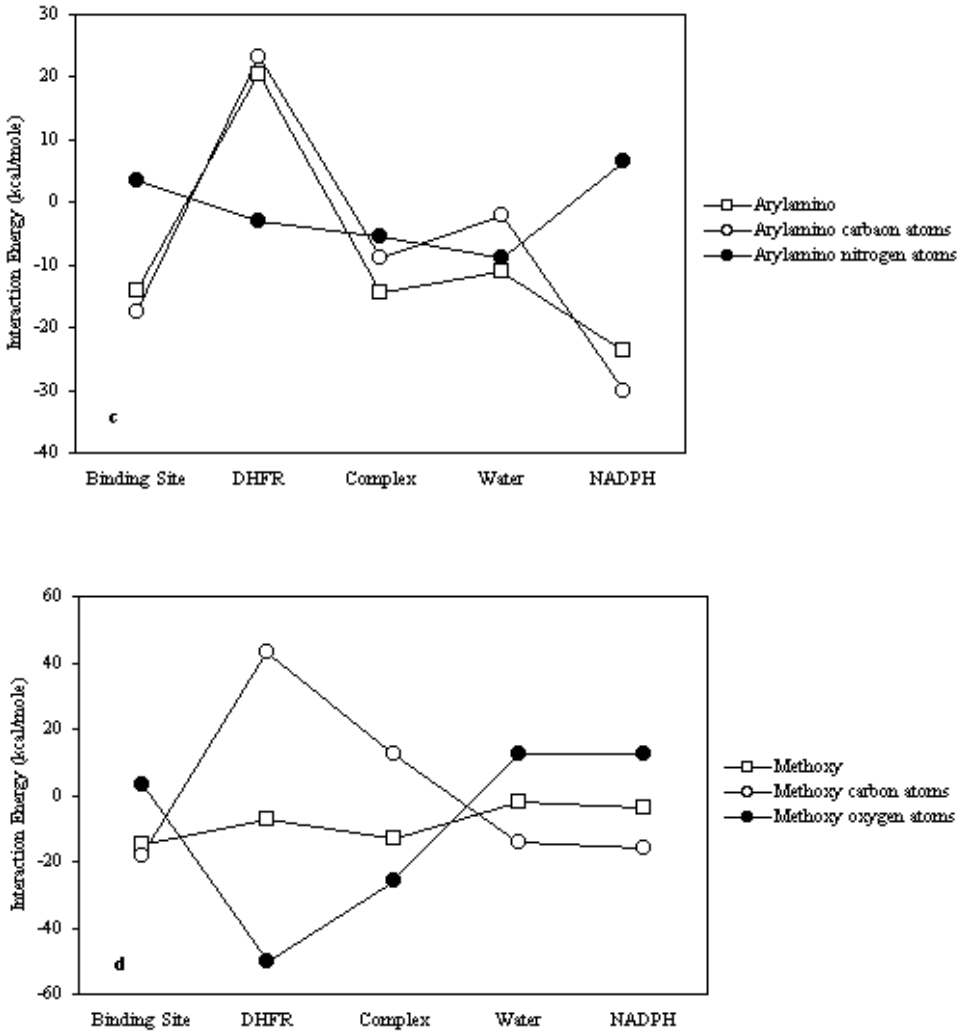

Figure 6 (continued) *Interaction energy analysis of TMQ and its substructural regions.* **c.** *Comparison of the arylamino region of TMQ with its carbon and nitrogen atoms.* **d.** *Comparison of the methoxy region of EPM with its carbon and nitrogen atoms*

gies may represent important targets for continued structural modification in the search for improved DHFR inhibitors.

Acknowledgements This work was supported in part by grants RCMI-NIH 5G12RR03048-13 and NIGMS-NIH S06GM0801628.

References

1. Schweitzer, B. I.; Dicker, A. P.; and Bertino, J. R.*FASEB J.* **1990**, *4*, 2441.
2. Allegra, C. J.; Kovacs, J. A.; Drake, J. C.; Swan, J. C.; Chabner, B. A.; Masur, H., *J. Exp. Med.* **1987**, *165*, 926.
3. Hamrell, M. R. *Oncology* **1984**, *41*, 343.
4. Bartlett, M. S.; Shaw, M.; Navaran, P.; Smith, J. W.; Queener, S. F. *Antimicrob. Agents Chemother.* **1995**, *39*, 2436.
5. Fulton, B.; Wagstaff, A. J.; McTavish D. *Drugs* **1995**, *49*, 563.
6. Marshall, J. L.; DeLap, R. *J.Clin Pharmacokinet.* **1994**, *26*, 190.
7. Takimoto, C. H, *Semin. Oncol.* **1997**, *24*, S18-40.
8. Mauritz, R.; Bekkenk, M. W.; Rots, M. G.; Pieters, R.; Mini, E.; van Zantwijk, C. H.; Veerman, A, J.; Peters, G. J.; Jansen, G. *Clin. Cancer Res.* **1998**, *4*, 2399.
9. Kim, J. S.; Lowe, K. E.; Shane, B. *J. Biol. Chem.* **1993**, *268*, 21680.
10. Kim, J. S.; Shane, B. *J. Biol. Chem.* **1994**, *269*, 9714.
11. Lowe, K. E.; Osborne, C. B.; Lin B. F.; Kin, J. S.; Hsu, J. C.; Shane, B. *J. Biol. Chem.* **1993**, *268*, 21665.
12. Clark, E. L.; Waxman, D. J.*Arch. Biochem. Biophys.* **1987**, *256*, 585.
13. Cook, J. D.; Cichowicz, D. J.; George, S.; Lawler, A.; Shane, B. *Biochemistry* **1987**, *26*, 530.
14. Scrimgeour, K. G. *Biochem. Cell Biol.* **1986**, *64*, 667.
15. Qi, H.; Atkinson, I.; Xiao, S.; Choi, Y. J.; Tobimatsu, T.; Shane, B. *Adv. Enzyme Regul.* **1999**, *39*, 263.
16. Takemura, Y.; Kobayashi, H.; Miyachi, H. *Int. J. Hematol.* **1997**, *66*, 459.

17. Rots, M. G.; Pieters, R.; Peters, G. J.; Noordhuis, P.; van Zantwijk, C. H.; Kaspers, G. J.; Hahlen , K.; Creutzig, U.; Veerman, A. J.; Jansen, G. *Blood* **1999**, *93*, 1677.
18. McCloskey, D. E.; McGuire, J. J.; Russell, C. A.; Rowan, B. G.; Bertino, J. R.; Pizzorno, G.; Mino, E. *J. Biol. Chem.* **1991**, *266*, 6181.
19. Baccanari, D. P.; Tansik, R. L.; Hitchings, G. H. *Adv. Enzyme Regul.* **1987**, *26*, 3.
20. Feun, L. G.; Robinson, W. A.; Savaraj, N.; Gonzalez, R.; Liebmann, A.; Offenhauser, K.; Clendeninn, N. J. *Am. J. Clin. Oncol.* **1995**, *18*, 488.
21. Bleechen, N. M.; Newman, H. V.; Rampling, R. P.; Ramsey, J. R.; Roberts, J. T.; Bedford, P.; Nethersell, A. B. *Br. J. Cancer* **1995**, *72*, 766.
22. Feun, L. G.; Savaraj, N.; Benedetto, P.; Waldman, S.; Collier, M.; Clendennin, N. J. *Am. J. Clin. Oncol.* **1994**, *17*, 448.
23. de Vries, E. G.; Gietema, J. A.; Workman, P.; Scott, J E.; Crawshaw, A.; Dobbs, H. J.; Dennis, I.; Mulder, N. H.; Sleijfer, D. T.; Willemse, P. H. *Br. J. Cancer* **1993**, *68*, 641.
24. Uen, W. C.; Huang, A. T.; Mennel, R.; Jones, S. E.; Spaulding, M. B.; Killion, K.; Keegan, P.; Clendeninn, N. *J.Cancer* **1992**, *69*, 1008.
25. Locher, H. H.; Schlunegger, H.; Hartman, P. G.; Angehrn, P.; Then, R. L. *Antimicrob. Agents Chemother.* **1996**, *40*, 1371.
26. Grem, J. L.; Voeller ,D. M.; Geoffroy, F.; Horak, E.; Johnston, P. G.; Allegra, C. J. *Br. J. Cancer* **1994**, *70*, 1075
27. Brun-Pascaud, M.; Chau, F.; Garry, L.; Jacobus, D.; Derouin, F.; Girard, P. M. *Antimicrob. Agents Chemother.* **1996**, *40*, 2067.
28. Martinez, A.; Allegra, C. J.; Kovacs, J. A. *Am. J. Trop. Med. Hyg.* **1996,** *54*, 249.
29. Chang, H. R.; Arsenijevic, D.; Comte, R.; Polak, A.; Then, R. L.; Pechere, J. C. *Antimicrob. Agents Chemother.* **1994**, *38*, 1803.
30. Lewis, W. S.; Cody, V.; Galitsky, N.; Luft, J. R.; Pangborn, W.; Chunduru, S. K.; Spencer, H. T.; Appleman, J. R.; Blakeley, R. L. *J. Biol. Chem.* **1995**, *270*, 5057.
31. Berman, H. M.; Westbrook, J.; Feng, Z.; Gilliland, G.; Bhat, T. N.; Weissig, H.; Shindyalov, I. N.; Bourne, P. E. *Nucleic Acids Res.* **2000**, *28*, 235.
32. QUANTA 97, Molecular Simulations Inc., San Diego, California, USA, 1997.
33. Jorgensen, W. L.; Chandrasekhar, J; Madura ,J. D.; Impey, R. W.; Klein, M. C. *J. Chem. Phys.* **1983**, *79*, 926.
34. Brooks, B. R.; Bruccoleri, R. E.; Olafson,B. D.; States, D. J.; Swaminathan, S.; Karplus, M. *J. Comput. Chem.* **1983**, *4*, 187.